PHYSICAL REVIEW B **81**, 172102 (2010)

Negative compressibility in platinum sulfide using density-functional theory

Arnaud Marmier,[1,*] Petros S. Ntoahae,[2] Phuti E. Ngoepe,[2] David G. Pettifor,[3] and Stephen C. Parker[4]
[1]*School of Engineering, Computer Science and Mathematics, University of Exeter, Exeter EX4 4QF, United Kingdom*
[2]*Material Modeling Centre, University of Limpopo, ZA-0727 Sovenga, South Africa*
[3]*Department of Materials, University of Oxford, Oxford OX1 3PH, United Kingdom*
[4]*Department of Chemistry, University of Bath, Bath BA2 7AY, United Kingdom*
(Received 21 August 2009; revised manuscript received 29 April 2010; published 19 May 2010)

The structural and dynamic properties of the mineral Cooperite (PtS) are investigated using density-functional theory. The results show that a competition with the less symmetric but more compact PdS structure leads to a phase transition when the pressure is increased. However, before the phase transition, PtS displays a rare anomalous elastic behavior by expanding along its long axis under hydrostatic pressure. We report the elastic constants of PtS and interpret this negative linear compressibility in the context of a displacive phase transition. We also show that the real structure of PtS is less symmetric than originally determined by experiment.

DOI: 10.1103/PhysRevB.81.172102 PACS number(s): 91.60.Ba, 61.50.Ks, 62.20.D−, 91.60.Gf

The interest in materials with abnormal elastic properties has been driven during the past decade by research into so-called auxetic materials.[1–3] Auxetic materials have a negative Poisson's ratio along one or more directions, which means that they respond to a longitudinal expansion by a lateral expansion (as opposed to the expected contraction). These materials were considered very rare,[4] but studies have proved that this property is far more common than expected, even in simple cubic metals.[5] While most current applications of auxetic materials[1,6] are at the macroscopic scale (polymeric or metallic foams), intriguing possibilities for nanoscopic and effectively incompressible structures exist, in the field of pressure sensors for instance.

Another very uncommon elastic property is exhibited by materials which display negative linear compressibility (NLC).[7] These materials, when submitted to hydrostatic pressure, contrary to intuition, do not contract in all directions but expand in at least one other direction. Very few (15) are currently known, among them are lanthanum niobates,[8] trigonal selenium,[9] and $Ag_3[Co(CN)_6]$.[10] Furthermore it seems unlikely that NLC can be as common as a negative Poisson's ratio because while the hydrostatic pressure is uniquely defined, strains can be applied in a great many directions (most negative Poisson's ratio result from strains in very specific directions). It is also important to note that the equation that governs linear compressibility is the transpose of that which controls volume change under pure normal stress and hence NLC materials are also stretch densified. Possible applications include zero compressibility composites, pressure sensors, or pressure driven actuators, as well as tunable sieves for filtration.

Platinum sulfide (PtS, also Cooperite) is a platinum-bearing mineral. As such, its properties relevant to platinum extraction are of interest to the mining industry, especially as economic mineral deposits become increasingly difficult to discover. Despite the possible technological interests, there has been little work on the structural aspects of PtS. We are not aware of any study of its surface structure and even its bulk phases have received little attention, with three experimental studies (two structural,[11,12] one concerned with high-pressure behavior[13]) and one computer simulation.[14]

In this Brief Report, we consider the structure, dynamics, and elastic properties of PtS as well as the structural changes under hydrostatic pressures up to 70 GPa. According to x-ray studies,[11,12] PtS belongs to the $P4_2/mmc$ space group (131). In this structure, containing four atoms per primitive cell, the S atoms occupy the corners of a tetragonally distorted simple cubic lattice, while the Pt atoms occupy the centers of two opposite faces of the cell, alternately in the (100) and (010) planes proceeding in the c direction. Platinum is coordinated to four sulfur atoms in a square planar arrangement, and sulfur is tetrahedrally coordinated to four platinum atoms (see Fig. 1). The figure shows that the large channels delimited by Pt-S bonds along the [100] and [010] directions are a distinctive feature of this structure. At a pressure of 3 GPa, Collins *et al.* observed a phase transition to a different structure, isomorphous to the palladium sulfide (PdS) structure[15] with a space group $P4_2/m$ (84) and 16 atoms per primitive cell. This last structure is less symmetric and denser than PtS, and while Pt and S retain their square planar and tetrahedral coordinations, there are half as many channels.

We simulate the PtS crystal within the framework of plane wave density-functional theory (PW DFT). For this, we use the VASP code[16–19] with two flavors of exchange-correlation functionals [PW cutoff of 500 eV, ultrasoft pseudopotentials,[20,21] local density approximation (LDA) and generalized gradient approximation (GGA) PW91 func-

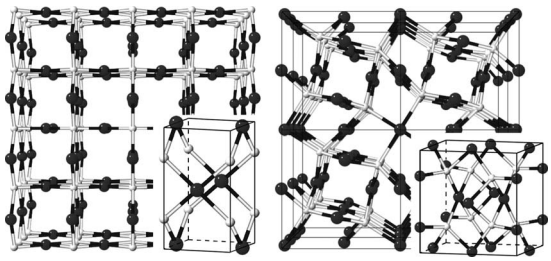

FIG. 1. (left) Structure of PtS, (right) Structure of PdS. Small white sphere represent sulfur atom, large black, platinum. In each case, the main figure shows a projection on the (001) plane, while the insert represents the primitive cell.

TABLE I. Structural and elastic properties of PtS/PdS. Formation energies are given per formula unit. Elastic constants in parentheses correspond to the new more stable structure (space group $P4_2/mnm$).

		Expt.	LDA	GGA
PtS structure	a (Å)	3.47[a,b]	3.44	3.54
	c (Å)	6.11[a,b]	6.09	6.17
	Atomic volume (Å^3)	18.4[a,b]	18.02	19.32
	E (eV)		−12.70	−10.61
PdS structure	a (Å)	6.43,[c] 6.41[b]	6.38	6.52
	c (Å)	6.66,[c] 6.60[b]	6.56	6.69
	Atomic volume (Å^3)	17.21,[c] 16.95[b]	16.69	17.77
	E (eV)		−12.71	−10.55
PtS structure	C_{11} (GPa)		217 (157)	186 (132)
	C_{12} (GPa)		73 (128)	53 (106)
	C_{13} (GPa)		149 (145)	113 (112)
	C_{33} (GPa)		343 (342)	283 (284)
	C_{44} (GPa)		30 (27)	28 (29)
	C_{66} (GPa)		12 (71)	13 (67)
	B (GPa)		169 (166)	135 (134)
	$C_{11}+C_{12}-2C_{13}$ (GPa)		−8 (−6)	13 (14)

[a]Reference 12.
[b]Reference 13.
[c]Reference 15.

tionals]. We shall refer to these functionals as LDA and GGA.

As the two structures types, referred to as PtS and PdS, have primitive cells containing a different number of atoms, we used a supercell for the smaller structure with the same number of atoms as the bigger structure (the $2\times2\times1$ supercell of the PtS structure is similar in size to the primitive cell of the PdS structure, see Table I) in order to benefit from error cancellations and from using comparable k-point meshes. We have found that Monkhorst-Pack k-point mesh of $5\times5\times5$ leads to the energy and lattice parameters being well converged. The resulting energy accuracy is around 10 meV per formula unit (5 meV per atom). The ionic positions and the cell parameters are relaxed using the Broyden-Fletcher-Goldfarb-Shanno optimizer.

The elastic constants are obtained from the direct approach of calculating the second order derivative of the energy for a set of strains.[22] We also calculated the phonon frequencies for some high-symmetry q points using the direct approach (frozen phonons).

Initially, we investigate the relative stability of the two structures by carrying out energy minimizations of the primitive PdS structure and of the comparable $2\times2\times1$ supercell of the PtS structure, without external pressure. The results are summarized in Table I. They follow the expected trend for LDA and GGA. The formation energies predicted by LDA for the two structures are sufficiently similar to be undistinguishable within our accuracy. LDA is well known to overbind and predict slightly shorter interatomic bonds and the platinum atoms modeled by LDA behave as if intermediate between real platinum and smaller palladium atoms. In contrast, the Pt atoms modeled by GGA are larger than the real atoms, and therefore a Pd-like structure is less stable. The real value for the energies and lattice constants are likely to be bracketed by those of the two functionals.

By using a $2\times2\times1$ supercell, we were also able to observe that the experimental structure is not the most stable. A new structure, of $P4_2/mnm$ space group (136), with a primitive cell twice the size of the original PtS structure and where the platinum atoms are slightly displaced, has a lower energy and hence is predicted to be the most stable form.

The existence of a less symmetric ground state for PtS is confirmed by frozen phonon calculations showing a soft mode at (0.5,0.5,0) (for a $1\times1\times1$ cell). The corresponding eigenvector is localized on the platinum atoms and leads to a displacement perpendicular to the plane formed by its four nearest-neighbor sulfur atoms (see PtS inset in Fig. 1). Calculation of the potential energy as a function of Pt displacement shows that the symmetric position (in plane) of the Pt atoms is a local maximum, and that there are minima either side. In addition, group theoretical considerations[23] preclude a $P4_2/mmc$ to $P4_2/m$ phase transition, while $P4_2/mnm$ to $P4_2/m$ is allowed (for the relevant q points).

From these calculations at zero pressure, we can draw three conclusions. The combination of functionals brackets the experimental lattice constants and respective stability of the PtS and PdS structure. The potential well for the Pt atom moving along a line perpendicular to the plane formed by its first shell of sulfur atoms is very flat. A structure with a primitive cell ($\sqrt{2}\times\sqrt{2}\times1$) and Pt atom distortion is more stable that the more symmetric structure (but may not be observed experimentally because the energy surface is flat and because of the local symmetry), and compatible with the experimentally observed phase transition.

We perform the same structural optimization, but under hydrostatic pressure up to 70 GPa. The structural behavior of

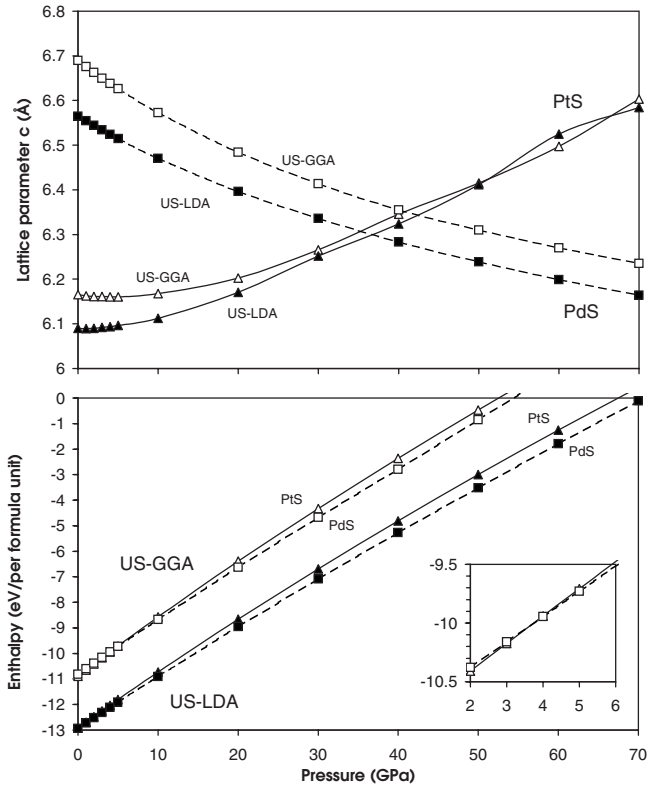

FIG. 2. Lattice parameters c (top) and enthalpy (bottom) of the PtS (triangle) and the PdS (square) structures as a function of pressure for LDA (broken line, empty symbols) and GGA (full line and symbols) calculations.

PtS under pressure is summarized in Fig. 2. As the volume decreases the conditions become more favorable for the more compact PdS structure. In the LDA case, the energetic advantage of this structure increases, while in the GGA case the PdS structure becomes stable at 4 GPa [this transition has been experimentally observed at 3 GPa (Ref. 13)].

The most striking feature of Fig. 2, which plots the enthalpy and lattice parameters of the PdS and PtS structures (in the more stable $P4_2/mnm$ crystal system), is the increase in the c parameter of the PtS structure with pressure, which does occur in all simulations. As discussed in the introduction, this is a very rare property. The linear compressibilities (defined as $-\Delta L/L\Delta P$, calculated between 0 and 10 GPa and between 10 and 20 GPa) are thus negative for the (001) direction, with values of -4.7×10^{-4} and -9.2×10^{-4} GPa^{-1} (LDA) and values of -8.0×10^{-5} and -6.4×10^{-4} GPa^{-1} (GGA). For comparison purposes, the normal positive linear compressibilities along the (100) direction are 3.3×10^{-3}, 3.1×10^{-3}, 3.6×10^{-3}, and 3.2×10^{-3} GPa^{-1}.

A simple consideration of the elastic constants can account for this abnormal behavior. A material of tetragonal symmetry will expand in the z direction while subjected to an isotropic pressure if $C_{11}+C_{12}-2C_{13}$ is negative[24] (the elastic constant tensor is represented here in the standard two-dimensional Voigt notation).

We calculated the elastic constants of platinum sulfide (restricting ourselves to the PtS structures, $P4_2/mmc$ and $P4_2/mnm$, and ignoring the PdS structure). As we are not aware of any experimental determination of the elastic properties of platinum sulfide, this information can also be used to further the development of atomistic models of this mineral. As can be seen in Table I, the sets of calculated elastic constants are quantitatively comparable (with the added subtlety, due to the orientation change, that C'_{11} must be compared to $\frac{1}{2}(C_{11}+C_{12})+C_{66}$, C'_{12} to $\frac{1}{2}(C_{11}+C_{12})-C_{66}$, and C'_{66} to $\frac{1}{2}(C_{11}-C_{12})$, where the unprimed and primed quantities corresponds to $P4_2/mmc$ and $P4_2/mnm$). However, the negative compressibility criterion ($C_{11}+C_{12}-2C_{13}<0$) is fulfilled in the LDA case, but not in the GGA case. A reanalysis of the pressure dependence of the GGA lattice parameters does indeed show that the linear compressibility along the long axis is positive, albeit very small until 3 Gpa.

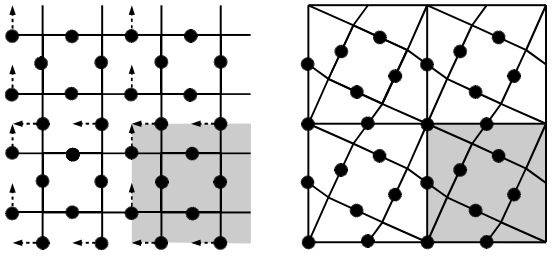

FIG. 3. Schematic illustration of the PtS to PdS phase transition, projected in the [001] plane, showing the linear densification. The segments represent S-Pt bonds (disks: Pt atoms; intersections: S atoms). In the left hand figure (PtS structure) the primitive cells appear as squares and a $2\times2\times1$ supercell is highlighted. The arrows indicate the Pt atoms displacements.

We postulate that the occurrence of negative linear compressibility is driven by the displacive (second order, where the order parameter is the Pt distance to its symmetric position at the center of a square, see the inset of Fig. 1) phase transition toward the PdS structure. Figure 3 presents a phenomenological interpretation and should be considered in conjunction with Fig. 1. It shows that the PdS structure can be obtained directly from a $2\times2\times1$ PtS supercell by internal quasi-rotation of $\pi/8$. We have already demonstrated that the potential well for such Pt displacements is initially very shallow. Such a modification conserves one of the channel units, but fills the other. More relevantly, due to the periodicity, the two platinum atoms from neighboring cells reach the same (projected) position. This results in a local linear densification, which can only be resolved by dilatation in the corresponding direction. This is also apparent in the experimental lattice constants (from Ref. 13, in Å) for the $2\times2\times1$ supercell of the PtS structure (6.94, 6.94, 6.11) and the PdS structure (6.41, 6.41, 6.59). These clearly indicate a compression in the [100] and [010] directions, but a dilatation in the [001] direction.

We would also like to point out that preliminary calculations on related crystals, platinum (II) oxide, PtO and PdO, with the same space group as Cooperite, predict a negative linear compressibility. In addition, empirical calculations based on a Keating model (simple bond hinges) also suggest that negative linear compressibility is a feature of the Cooperite structure.

We have studied the structural and elastic properties of

platinum sulfide. We show that neither LDA nor GGA is ideal, but that they bracket the property of the material. We also suggest that the structure of PtS belongs to the less symmetric $P4_2/mnm$ space group. This structure is not only shown to be more stable by calculations, but it is also compatible with the experimentally observed phase transition toward $P4_2/m$ (while $P4_2/mmc$ is not). Finally, we observe that the PtS structure (in both $P4_2/mmc$ and $P4_2/mnm$ space groups) expands along the (001) direction when subjected to hydrostatic pressure, and this whichever the functional. This lack of dependence on the functional, coupled with a phenomenological interpretation of the phase transition and interpretation of the experimental lattice parameters, gives us confidence in the result. While materials that exhibit this kind of negative compressibility are not entirely unknown, they are nevertheless very rare.

*Corresponding author.

[1] R. H. Baughman, Nature (London) **425**, 667 (2003).
[2] R. H. Baughman *et al.*, Science **288**, 2018 (2000).
[3] K. E. Evans *et al.*, Nature (London) **353**, 124 (1991).
[4] N. R. Keskar and J. R. Chelikowsky, Nature (London) **358**, 222 (1992).
[5] R. H. Baughman *et al.*, Nature (London) **392**, 362 (1998).
[6] K. E. Evans and A. Alderson, Adv. Mater. **12**, 617 (2000).
[7] R. H. Baughman *et al.*, Science **279**, 1522 (1998).
[8] J. W. E. Mariathasan, L. W. Finger, and R. M. Hazen, Acta Crystallogr., Sect. B: Struct. Sci. **41**, 179 (1985).
[9] R. W. Munn, J. Phys. C **5**, 535 (1972).
[10] A. L. Goodwin, D. A. Keen, and M. G. Tucker, Proc. Natl. Acad. Sci. U.S.A. **105**, 18708 (2008).
[11] F. A. Bannister and M. H. Hey, Miner. Mag. **23**, 188 (1932).
[12] F. Grønvold, H. Haraldsen, and A. Kjekshus, Acta Chem. Scand. **14**, 1879 (1960).
[13] R. Collins *et al.*, Inorg. Chem. **18**, 727 (1979).
[14] P. Raybaud *et al.*, J. Phys.: Condens. Matter **9**, 11085 (1997).
[15] F. Grønvold and E. Røst, Acta Chem. Scand. **10**, 1620 (1956).
[16] G. Kresse and J. Hafner, Phys. Rev. B **47**, 558 (1993).
[17] G. Kresse and J. Hafner, Phys. Rev. B **49**, 14251 (1994).
[18] G. Kresse and J. Furthmüller, Comput. Mater. Sci. **6**, 15 (1996).
[19] G. Kresse and J. Furthmüller, Phys. Rev. B **54**, 11169 (1996).
[20] D. Vanderbilt, Phys. Rev. B **41**, 7892 (1990).
[21] G. Kresse and J. Hafner, J. Phys.: Condens. Matter **6**, 8245 (1994).
[22] O. Beckstein *et al.*, Phys. Rev. B **63**, 134112 (2001).
[23] H. T. Stokes and D. M. Hatch, *Isotropy Subgroups of the 230 Crystallographic Space Groups* (World Scientific, Singapore, 1988).
[24] J. F. Nye, *Physical Properties of Crystals* (Clarendon Press, Oxford, 1985).